International Journal of Pharmaceutics 399 (2010) 109–115

Contents lists available at ScienceDirect

International Journal of Pharmaceutics

journal homepage: www.elsevier.com/locate/ijpharm

A thermal analysis method to predict the complete phase diagram of drug–polymer solid dispersions

Dexi Lin, Yanbin Huang*

Department of Chemical Engineering, Tsinghua University, Beijing 100084, China

ARTICLE INFO

Article history:
Received 11 May 2010
Received in revised form 4 August 2010
Accepted 11 August 2010
Available online 18 August 2010

Keywords:
Solid dispersion
The Flory–Huggins theory
Phase diagram
Phase separation
Felodipine/PAA system

ABSTRACT

The aim of this work was to develop a method which uses experimentally obtainable data to predict the complete phase diagram of drug–polymer solid dispersion systems, for the first time in literature. Felodipine–poly(acrylic acid) (PAA) solid dispersion was used as an example to illustrate the application of this method. Samples were prepared with different drug loading and analyzed using differential scanning calorimetry (DSC). Values of the drug–polymer interaction parameter $\chi(T_m)$ were calculated from the drug crystal melting point depression data. Since χ is a function of temperature ($\chi \sim 1/T$) according to the Flory–Huggins theory, the obtained χ–T relationship thus enabled calculation of the complete temperature-composition phase diagram of a drug–polymer solid dispersion system. In experiments, felodipine was shown to be immiscible with PAA in almost the whole range of drug content at room temperature. Two glass transition temperatures were observed, corresponding to almost pure felodipine and pure PAA, respectively, in consistent with the predicted phase behavior.

1. Introduction

The enhancement of bioavailability of poorly water-soluble drugs is one of the most challenging problems in pharmaceutical science. Drug–polymer solid dispersion can markedly improve the dissolution rate of drugs and lead to higher bioavailability (Chiou and Riegelman, 1971; Leuner and Dressman, 2000; Yu, 2001). However, due to the lack of miscibility between most of the insoluble drugs and commonly used hydrophilic polymers, drug tends to crystallize out of the initially homogeneous drug/polymer solution during storage, especially at high drug loading and/or when exposed to moisture (Serajuddin, 1999; Vasconcelos et al., 2007; Rumondor et al., 2009a; Marsac et al., 2010). Besides drug crystallization, amorphous phase separation may also take place (Friesen et al., 2008; Janssens and Van den Mooter, 2009) and generate drug-rich and polymer-rich amorphous domains, which are still thermodynamically unstable in comparison with drug crystal. Hence, crystallization may start from these amorphous domains instead of the homogeneous drug/polymer solution (Six et al., 2003; Vasanthavada et al., 2005; Rumondor et al., 2009c). In addition, both crystallization and amorphous phase separation may be interrupted by the glass transition (Cheng, 2008; Qian et al., 2010). Therefore, for an apparently simple drug–polymer two-component system, it can go through multiple phase separation pathways and kinetically trapped in different metastable points in the temperature-composition phase diagram. Consequently, the drug dispersion structures may vary depending both on the composition and the thermal treatment history of the solid dispersion systems. Therefore, it is highly desirable to construct a complete phase diagram as a map where the possible phases of a solid dispersion system can be located, including the liquid–solid phase transition curve (i.e., the crystallization curve, along which drug crystals coexist with a drug/polymer glass solution in equilibrium), the amorphous phase separation curves, and the glass transition curve.

Based on the polymer solution theory, a typical phase diagram of a small molecule–polymer system looks like Fig. 1, including the liquid–solid phase transition curve, the bimodal and spinodal amorphous phase separation curves, and the glass transition temperature (T_g) curve (Cheng, 2008).

The liquid–solid transition curve represents the equilibrium solubility of drug crystals in the polymer matrix at different temperatures. The area above this curve means that drugs are dissolved in polymer and form an unsaturated solution, while the area below means that the drug loading in the solid dispersion is above its equilibrium solubility, and drug molecules tend to precipitate out as drug crystals which exist in equilibrium with a drug/polymer solution whose composition is determined by the liquid–solid phase transition curve.

As first proposed by Mohan et al. (2002) and later applied to solid dispersion systems by Taylor's and Yu's groups (Marsac et al., 2006, 2009; Tao et al., 2009), this liquid–solid transition curve can be determined via differential scanning calorimetry (DSC) mea-

* Corresponding author. Tel.: +86 10 6279 7572.
E-mail address: yanbin@tsinghua.edu.cn (Y. Huang).

0378-5173/$ – see front matter © 2010 Elsevier B.V. All rights reserved.
doi:10.1016/j.ijpharm.2010.08.013

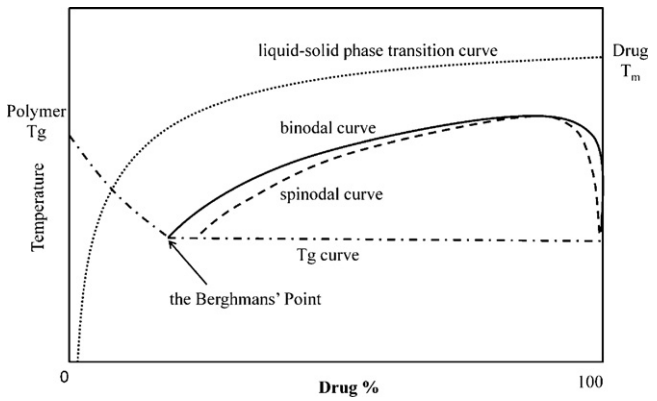

Fig. 1. A theoretical phase diagram of drug–polymer solid dispersions based on the polymer solution theory (Koningsveld et al., 2001).

surement through the end points of the melting peaks. However, as pointed out previously (Marsac et al., 2006; Qian et al., 2010), only part of the curve at temperatures above T_g could be obtained experimentally, because of the high viscosity at lower temperatures and the difficulty for the system to reach equilibrium.

When the system is cooled to temperature below the liquid–solid phase transition curve, amorphous (liquid–liquid) phase separation may take place prior to drug crystallization, and amorphous polymer-rich and drug-rich phases are formed (Cheng, 2008). Here drug crystallization represents the thermodynamically stable state, while amorphous phase separation represents the metastable states.

As shown in Fig. 1, the amorphous phase separation is defined by two curves. The binodal curve represents the metastable amorphous phase separation line (polymer-rich and drug-rich phases coexist with each other), while the spinodal curve represents a change in the mechanism of amorphous phase separation (Rubinstein and Colby, 2003; Cheng, 2008): for systems within the area between the binodal and spinodal curves, amorphous phase separation goes through a nucleation & growth pathway, where the drug-rich domains first form as small droplets and grow in size; on the other hand, for systems below the spinodal curve, amorphous phase separation forms bicontinuous polymer-rich and drug-rich domains at first and then goes through a coarsening process. Classical polymer textbooks (e.g., Strobl, 2007) have more information on the amorphous phase separation mechanisms and their phase structure evolution. In principle, these transient phase structures could be fixed by cooling down the sample below the glass transition temperature, and this provides our motivation to study the phase diagram as a guiding map for future studies.

The glass transition is not a real phase transition, but it is very important for phase separation kinetics and structure formation (Cheng, 2008). The glass transition curve can be easily determined via DSC measurement. Several studies in literatures observed or implied two glass transition temperatures in their solid dispersion samples, indicating amorphous phase separation (Wiranidchapong et al., 2008; Gashi et al., 2009; Rumondor et al., 2009a,b). However, no systematic study on the amorphous phase separation curves was reported. Light scattering is a classical method to experimentally determine the amorphous phase separation curves (Koningsveld et al., 2001), but a prediction of their approximate locations will significantly simplify the experiment design. The glass transition temperature curve and the Berghmans' Point will be discussed in more detail in Section 2.4.

According to the Flory–Huggins polymer solution theory (Flory, 1953), the drug–polymer temperature-composition phase diagram can be predicted if we know how the drug–polymer interaction parameter χ changes with temperature (it should be noted that, in the Flory–Huggins theory, χ is a function of temperature only). Marsac et al. (2006, 2009) first used the melting point depression data to predict χ by using Eq. (1):

$$\frac{1}{T_m} - \frac{1}{T_m^0} = -\frac{R}{\Delta H}\left(\ln\phi + \left(1 - \frac{1}{m}\right)(1-\phi) + \chi(1-\phi)^2\right) \quad (1)$$

where T_m and T_m^0 are the melting temperatures of the drug crystal in drug/polymer mixtures and the pure drug, respectively, R is the gas constant, ΔH is the heat of fusion of the pure drug, ϕ is the volume fraction of the drug and m is the ratio of the volume of a polymer chain to that of a lattice site (defined here as the volume of a drug molecule), χ is the drug–polymer interaction parameter. In their work, interaction parameter was calculated as a constant, but according to the Flory–Huggins theory (Flory, 1953) and as recently pointed out by Janssens and Van den Mooter (2009) and Qian et al. (2010), χ is a function of temperature which can be empirically described by Eq. (2) (Rubinstein and Colby, 2003):

$$\chi = A + \frac{B}{T} \quad (2)$$

where A and B are constants. Eq. (2) is the widely used empirical expression for χ, where A is referred to as the non-combinatorial entropic contribution to χ, while B/T is the enthalpic contribution (Rubinstein and Colby, 2003, p. 145). By using Eq. (2), we neglected the possible dependence of χ on drug concentration and higher terms of T (e.g., T^2). In the Flory–Huggins theory, χ represents the interaction between polymer segments and drug molecules. A negative χ means that the attraction between a polymer–drug pair is stronger than the average attraction between a polymer–polymer pair and a drug–drug pair (i.e., drug–polymer > 1/2(drug–drug + polymer–polymer)), so drug molecules prefer to be in contact with polymer segments than with other drug molecules. Values of χ become more negative when this preference becomes stronger. On the other hand, a positive χ means drug molecules and polymer segments prefer to be in contact with those of their own kind rather than mixing with each other. The key point of our method is to realize that the χ values obtained from the melting point depression data via Eq. (1) correspond to those at temperature T_m. Thus, by measuring melting points of drugs in solid dispersion at different drug/polymer ratios, we can actually obtain a series of χ values at different T_m. By plotting the $\chi \sim 1/T$ data according to Eq. (2), we can obtain parameters A and B and then predict χ at any temperature. Afterwards, the complete phase diagram can be predicted within the framework of the Flory–Huggins theory.

In the following, we will use the felodipine–poly(acrylic acid) (PAA) system to exemplify how a complete phase diagram can be predicted from data obtained through thermal analysis. The felodipine–PAA system was chosen because it was previously demonstrated by Rumondor et al. (2009b) to show amorphous phase separation.

2. Materials and methods

2.1. Materials

Felodipine was a generous gift from Hefei Cubic Pharmaceutical Company (Anhui, China). Poly(acrylic acid) (PAA, average $M_w \approx 1800$) was purchased from Sigma–Aldrich (Batch # 117K5055).

2.2. Sample preparation

PAA was dried in a desiccator over phosphorus pentoxide powder for at least 1 week before use. Felodipine and PAA with different weight ratios (total weight 0.5 g) were dissolved in 20 ml ethanol

and stirred for 24 h to ensure complete dissolution. The solvent was then removed using a rotary evaporator. Samples were collected and subsequently further dried under vacuum at 50 °C for 24 h to remove residual solvent. The resulting material was milled gently with a pestle and mortar, passed through a mesh-100 filter, and stored in a desiccator over phosphorus pentoxide powder at room temperature before test. Two sets of samples were prepared at each concentration.

2.3. Melting point measurement

The melting temperature of felodipine in the solid dispersion was measured with DSC (SHIMADZU DSC-60). The instrument was calibrated for temperature and enthalpy measurement by using indium and zinc. Before measurement, samples were first annealed under vacuum at 100 °C for 2.5 h to promote drug crystallization in the sample. The annealing temperature was chosen to be 100 °C because it is close to the glass transition temperature of poly(acrylic acid) in order to facilitate drug crystallization. In the DSC test, samples were first heated to 110 °C at a scan rate of 10 °C/min, and then continue to 155 °C at a scan rate of 1 °C/min to obtain the melting temperature value as close to the equilibrium one as possible (Tao et al., 2009). The end points of melting were calculated from DSC thermograms as the intersection of the falling edge of the melting endotherm and the post-melting baseline.

The glass transition temperatures were measured with a TA Instrument DSC Q2000, whose temperature calibration was done by using indium. Samples were pre-heated in the DSC pan to 160 °C, cooled to 0 °C, and reheated to 120 °C (all with a scan rate of 10 °C/min).

2.4. Method development

2.4.1. Melting point depression and the relationship between χ and T

Melting of a pure drug occurs at the temperature when the chemical potential of the crystalline drug is equal to the chemical potential of the drug melt. If the melt drug is miscible with a polymer and dissolved in it, the chemical potential of the drug in the solution will be lower than that of the pure drug melt, and this phenomenon leads to melting point depression of drug crystals embedded in the polymer matrix (Marsac et al., 2009), as described by Eq. (1). As somehow overlooked by the previous studies and recently pointed out by Janssens and Van den Mooter (2009) and Qian et al. (2010), χ is a function of temperature (Eq. (2)). Taking a closer look at the derivation of Eq. (1), χ is actually corresponding to the interaction parameter at T_m. Thus, from melting point depression measurement of samples with different drug loading, we can obtain interaction parameter values at different temperatures, and use Eq. (2) to get A and B by a linear fit of χ vs. $1/T$.

2.4.2. Prediction of the complete liquid–solid phase transition curve

After knowing A and B, we can calculate the interaction parameters at other temperatures. Thus, the complete liquid–solid phase transition curve can be constructed using Eq. (1), and we can predict the equilibrium drug solubility in polymer at temperatures below T_g, which cannot be obtained experimentally (Tao et al., 2009; Qian et al., 2010).

2.4.3. Prediction of the amorphous phase separation curves

According to the Flory–Huggins theory, the free energy of mixing for drug–polymer solid dispersion can be described by Eq. (3):

$$\Delta G = RT\left[\phi\ln\phi + \frac{1-\phi}{m}\ln(1-\phi) + \chi\phi(1-\phi)\right] \quad (3)$$

Table 1
Parameters used to calculate interaction parameter and the free energy of mixing.

	M_w (g/mol)	Density (g/cm^3)
Felodipine	384.26	1.28 (Marsac et al., 2006)
PAA	1800	1.27 (Yu et al., 2006)

Then, the spinodal phase separation curve ($T_s - \phi$) can be calculated by equating the second derivative of the free energy to zero and expressed as (Eq. (4)):

$$T_s = \frac{2B}{(1/\phi) + (1/(m(1-\phi))) - 2A} \quad (4)$$

The phase boundary (the binodal phase separation curve $T_b - \phi$) is determined by the common tangent of the free energy at the compositions ϕ' and ϕ'' corresponding to the two phases resulted from the amorphous phase separation:

$$\left(\frac{\partial\Delta G}{\partial\phi}\right)_{\phi=\phi'} = \left(\frac{\partial\Delta G}{\partial\phi}\right)_{\phi=\phi''} \quad \text{at} \quad T_b \quad (5)$$

Eq. (5) can be solved with a simple computer program. For more details, please see Rubinstein and Colby (2003).

Table 1 shows the parameters used to calculate χ according to Eq. (1), the ratio of the volume of a polymer chain to that of a lattice site (defined here as the volume of a drug molecule) can be calculated by Eq. (6):

$$m = \frac{M_w(\text{PAA})/\rho(\text{PAA})}{M_w(\text{felodipine})/\rho(\text{felodipine})} \quad (6)$$

2.4.4. The significance of the Berghmans' Point

Fig. 1 shows the theoretical phase separation curves of a drug–polymer system with an upper critical solution temperature (UCST) behavior (Koningsveld et al., 2001; Cheng, 2008). At high temperatures, the two components are miscible, and there is a single T_g for the system, usually described by the Fox Equation:

$$\frac{1}{T_g} = \frac{\omega_1}{T_{g1}} + \frac{\omega_2}{T_{g2}} \quad (7)$$

where ω_i and T_{gi} are the weight fraction and glass transition temperature of each component i, respectively. When the temperature is lowered, the liquid–liquid phase separation may take place first before crystallization, as the former has a lower energy barrier to overcome than the latter (Janssens and Van den Mooter, 2009; Qian et al., 2010). After amorphous phase separation, the system is divided into polymer-rich and drug-rich phases, and the volume fractions of the individual components within the two phases are determined by the tie line end points on the binodal curve at a given temperature. Consequently, the two phases will have two separate T_gs corresponding to the $T_g - \phi$ relationship (Eq. (7)). The region between the binodal and spinodal curves is the metastable region where phase separation must overcome a nucleation barrier to grow, while within the spinodal zone amorphous phase separation proceeds spontaneously (Rumondor et al., 2009b).

If the glass transition curve intersects the binodal curve, as shown in Fig. 1, the intersection is called the Berghmans' Point in polymer literature (Arnauts and Berghmans, 1987). When the temperature is lowered below that of the Berghmans' Point, one phase reaches its glass transition point, and then the phase separation process along with the composition changes will be kinetically stopped. Consequently, the two observed glass transition temperatures do not change with the initial drug concentration, i.e., the composition of the two arrested phases are always the same (Cheng, 2008). However, the relative volume ratios of the two phases vary with the initial drug concentration. These are well described in the polymer science literature (Cheng, 2008).

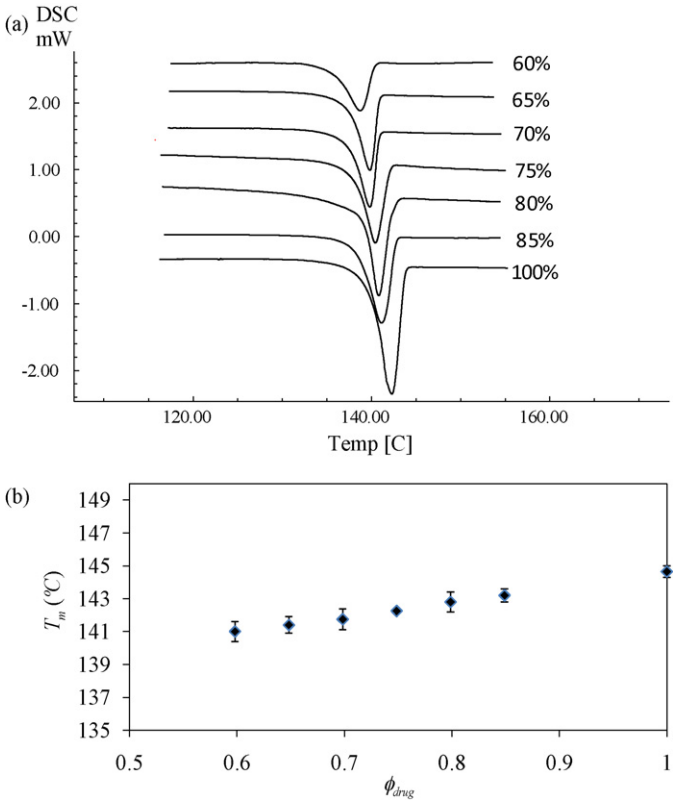

Fig. 2. (a) DSC thermograms of felodipine–PAA solid dispersion measured at a heating rate of 1 °C/min, and the numbers on each curve indicates the drug loading in weight percentage; (b) melting temperatures T_m of felodipine as a function of drug loading (volume fraction) in the solid dispersion. The data were the average from two separate sample preparations and measurements.

3. Results and discussion

3.1. Melting point depression and the relationship between χ and T

Since it was first proposed by Mohan et al. (2002), DSC has been used to measure the equilibrium solubility of drugs in small molecule solvents and polymers. This method involves heating a crystal/solvent system of certain composition (ϕ). The key point (Mohan et al., 2002; Tao et al., 2009) is to realize that the solubility of the crystal in the solvent is exactly ϕ at the final temperature of crystal dissolution, which is calculated as the intersection of the tangents on the heat flow peak (T_{end}). Here we use this method to measure the solubility of felodipine in PAA, and the results obtained are shown in Fig. 2. The data in Fig. 2b were the average between two sets of samples, prepared and measured separately, and these data were used for the analysis below. As pointed out by Tao et al. (2009), ideally T_{end} should be measured at different heating rates and extrapolated to zero heating rate in order to obtain its true equilibrium value. In our experiments, we used a low molecular weight PAA ($M_w \approx 1800$) with low viscosity, and chose a heating rate of 1 °C/min but did not choose a lower rate due to concerns over PAA and felodipine degradation in a longer heating process.

As shown in Fig. 3, the plot of χ vs. $1/T$ is generally linear, consistent with Eq. (2), and the values of A and B are -18.84 and 8.105×10^3 K, respectively. When calculating the interaction parameter, it should be emphasized that: (1) χ is very sensitive to the T_{end} values when the drug content is high (above 90%). According to Eq. (1), as the drug content approaches 100%, χ scales to $1/(1-\phi)^2$ (which is approaching to infinity), and this means a small

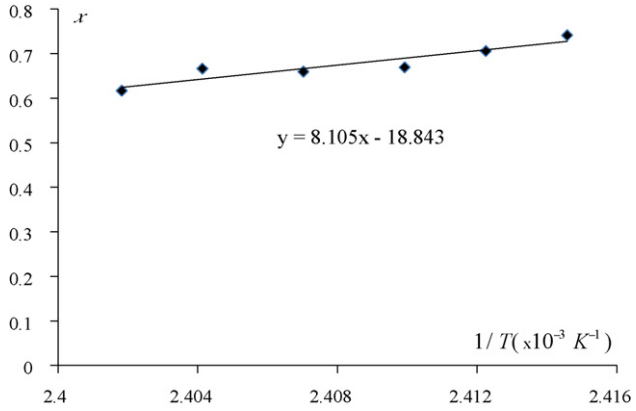

Fig. 3. Linear fit of interaction parameter and $1/T$ based on Eq. (1) to calculate A and B.

change of temperature measured can lead to a great change of χ; (2) only those solid dispersions with detectable drug crystal contents can be used to determine χ. In our experiment, no melting peak was observed for samples with 30 wt% or lower. In addition, the system is hard to reach equilibrium for samples with high polymer content due to their high viscosity. In our work, we chose solid dispersion with drug contents between 60 and 85 wt% to determine the $\chi - T$ relationship; (3) this method is only valid within the framework of the Flory–Huggins theory. For example, many polymer–polymer blend systems have the interaction parameters not only dependent on T, but also on the compositions (Han et al., 1988; Rubinstein and Colby, 2003), which is not considered in our method; (4) there is an implicit assumption in deriving Eq. (1): the drug–polymer mixture above T_m is a homogeneous solution, i.e., no amorphous phase separation occurs above T_m.

3.2. Phase diagram construction

Fig. 4 shows the predicted complete liquid–solid phase transition curve. The extent of melting point depression for felodipine in PAA is little for almost the whole composition range. At room temperature of 25 °C, the predicted equilibrium solubility of felodipine in PAA is less than 0.1 wt% (3.17×10^{-4} wt%).

Fig. 5a shows the typical results from DSC measurement to determine the glass transition temperatures. The small endothermic peak prior to the major melting peak was possibly due to the melting of drug crystals of smaller size. During the first heating

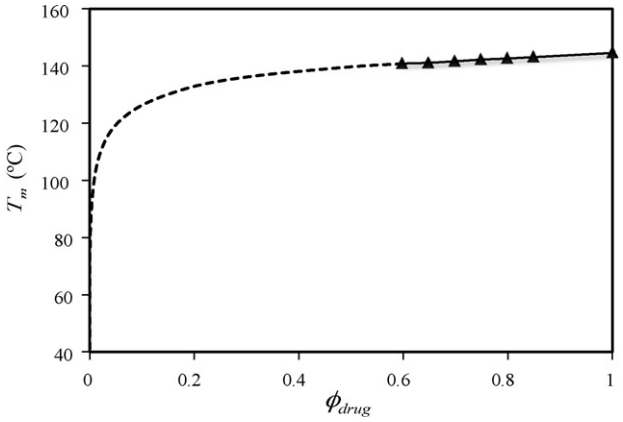

Fig. 4. Complete liquid–solid phase transition curve for the felodipine–PAA system. The dashed line is predicted based on Eq. (1) and Eq. (2), and the solid triangles represent experimental results.

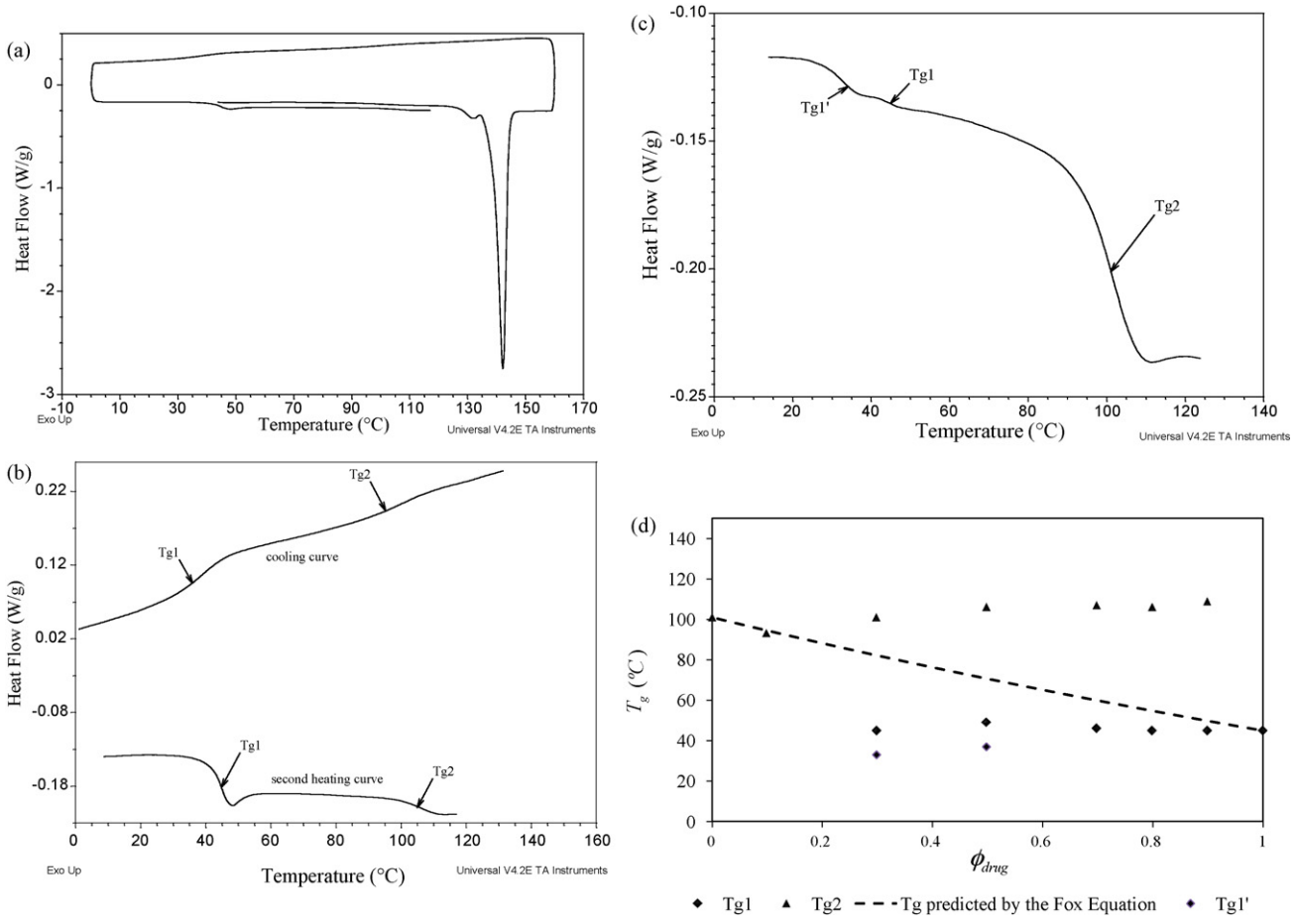

Fig. 5. DSC thermograms of solid dispersion sample with 80 wt% felodipine, including the first heating, the subsequent cooling, and the second heating scan, all measured at a heating rate of 10 °C/min (a); The magnified cooling and reheating curves from (a), T_{g1} is 45 °C and T_{g2} is 106 °C in the second heating measurement (b); DSC thermograms of solid dispersion sample with 30 wt% felodipine measured at a heating rate of 10 °C/min (the reheating curve), T'_{g1} is 33 °C and T_{g1} is 45 °C (c); T_gs of felodipine–PAA amorphous mixture (d).

scan, melting of felodipine crystals was observed, while no crystallization peak was observed in the subsequent cooling scan. Instead, two glass transitions were detected in the cooling scan as well as in the second heating scan (Fig. 5b), indicating amorphous phase separation took place during cooling instead of drug crystallization. Similar results were obtained for samples with drug contents from 30 to 90 wt% as plotted in Fig. 5d together with the predicted T_g curve from Eq. (7). However, for the samples containing 30 and 50 wt% felodipine, one more T_g below the glass transition temperature of pure felodipine was observed (Fig. 5c). This lower T_g of felodipine was also observed by Karavas et al. (2005). In their experiments for felodipine–PVP system, the T_g of drug-rich phase for 25 wt% felodipine and 50 wt% felodipine samples were 37.6 and 30.1 °C, respectively. The reasons are still unclear to us.

The complete phase diagram for the felodipine–PAA system is calculated based on the aforementioned method, including the liquid–solid phase transition curve, the binodal and spinodal amorphous phase separation curves (Fig. 6). Felodipine was found immiscible with PAA in almost the whole range of drug content at temperatures below 100 °C, and the predicted Berghmans' Point is at the position with drug content of 2.94 wt% (i.e., almost pure polymer) and temperature at 99.1 °C. As temperatures being lowered than 100 °C, amorphous phase separation would take place and the system would be separated into two phases with compositions corresponding to almost pure felodipine and PAA, respectively. As

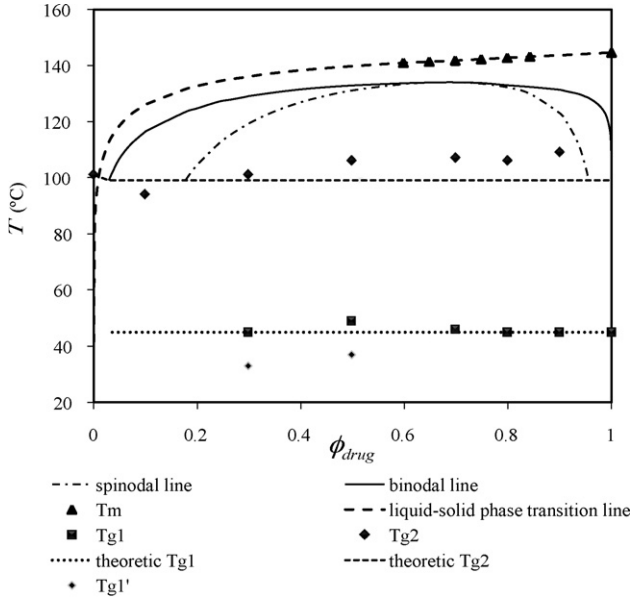

Fig. 6. Complete phase diagram predicted for the felodipine–PAA system.

discussed before, we should observe two T_gs equal to the glass transition temperatures of almost pure felodipine and PAA. This is consistent with our experiment observation (Fig. 6) and what Rumondor et al. (2009b) observed with PAA of higher molecular weight. It should be noted that for the sample containing 10 wt% felodipine, only one T_g was observed, even though amorphous phase separation was predicted for this composition. The cause for this apparent discrepancy was not clear, but a possible reason is that the sample with this drug content is in the region between the binodal and spinodal lines according to Fig. 6, where the phase separation must overcome a nucleation barrier. Coupled with the high viscosity of this system with 90% polymer, the phase separation may be kinetically prevented during cooling. Alternatively, this may also be beyond the accuracy limit of our proposed method to this specific system.

It should be noted that: (1) the method could not explain why most of other drug/polymer solid dispersion systems in literature did not show amorphous phase separation (i.e., two glass transition temperatures are rarely observed in literature), which may be due to the kinetics of competing phase separation pathways (crystallization vs. amorphous phase separation). In our next step, we will use light scattering to further study the phase separation kinetics to clarify this problem and other issues above; (2) due to high viscosity of the polymer systems, the equilibrium melting point of drug crystals in polymer matrix is very difficult to determine precisely in reality (Tao et al., 2009), and this makes the prediction of interaction parameters even more challenging.

4. Conclusions

In this paper, we proposed a method to predict the temperature-composition phase diagram of drug/polymer solid dispersion. The proposed method is based on the Flory–Huggins polymer theory and includes the following steps: (1) preparing drug/polymer solid dispersion samples of different drug loading, (2) using DSC to determine the melting temperatures of drug crystals in these samples and hence obtain the T_m – drug loading ϕ relationship, (3) using the melting point depression equation (Eq. (1)) derived from the Flory–Huggins theory to calculate the drug–polymer interaction parameters χ corresponding to T_m, (4) using these obtainable $\chi - T$ data to fit the empirical $\chi - T$ relationship (Eq. (2)) and hence to obtain the complete $\chi - T$ equation, (5) using the $\chi - T$ equation to predict χ values at other temperatures, and afterwards the complete phase diagrams of the drug/polymer system can be predicted by using the Flory–Huggins polymer theory including the liquid–solid phase transition curve (Eq. (1)) and the amorphous phase separation curves (Eqs. (4) and (5)).

We used a felodipine/PAA system to illustrate how the proposed method is used. The results predicted that the equilibrium solubility of felodipine in PAA is below 0.1 wt%. It should be noted that equilibrium solubility of drug in polymer at temperature below the glass transition temperature could not be experimentally determined, and this method provided a way to predict them. In addition, our method predicted that the felodipine/PAA system, if amorphous phase separated, would form a phase of almost pure drug and the other phase of almost pure polymer. This prediction was consistent with the two T_gs measured in experiments.

It should be emphasized again that the current method relies heavily on the Flory–Huggins polymer theory, and hence its validity and accuracy are within the boundary of the latter. Also, the prediction accuracy is also dependent on how accurate the melting point depression data can be obtained in experiments, and currently there is no consensus on which experimental protocol could determine the equilibrium melting temperature of drug crystals in polymer matrix (Sun et al., 2010). Therefore, the phase diagram predicted by the current method should be considered a rough draft, rather than an accurate one.

Acknowledgments

This work was supported by National Natural Science Foundation of China (Project No. 50743038 and No. 50873056).

References

Arnauts, J., Berghmans, H., 1987. Amorphous thermoreversible gels of atactic polystyrene. Polym. Commun. 28, 66–68.
Cheng, S.Z.D., 2008. Phase Transitions in Polymers: The Role of Metastable States. Elsevier, Amsterdam.
Chiou, W.L., Riegelman, S., 1971. Pharmaceutical applications of solid dispersion systems. J. Pharm. Sci. 60, 1281–1302.
Flory, P.J., 1953. Principles of Polymer Chemistry. Cornell University Press, Ithaca.
Friesen, D.T., Shanker, R., Crew, M., Smithey, D.T., Curatolo, W.J., Nightingale, J.A.S., 2008. Hydroxypropyl methylcellulose acetate succinate-based spray-dried dispersions: an overview. Mol. Pharm. 5, 1003–1019.
Gashi, Z., Censi, R., Malaj, L., Gobetto, R., Mozzicafreddo, M., Angeletti, M., Masic, A., Martino, P.D., 2009. Differences in the interaction between aryl propionic acid derivatives and poly(vinylpyrrolidone) K30: a multi-methodological approach. J. Pharm. Sci. 98, 4216–4228.
Han, C.C., Bauer, B.J., Clark, J.C., Muroga, Y., Matsushita, Y., Okada, M., Tran-cong, Q., Chang, T., Sanchez, I.C., 1988. Temperature, composition and molecular-weight dependence of the binary interaction parameter of polystyrene/poly(vinyl methyl ether) blends. Polymer 29, 2002–2014.
Janssens, S., Van den Mooter, G., 2009. Review: physical chemistry of solid dispersions. J. Pharm. Pharmacol. 61, 1571–1586.
Karavas, E., Ktistis, G., Xenakis, A., Georgarakis, E., 2005. Miscibility behavior and formation mechanism of stabilized felodipine–polyvinylpyrrolidone amorphous solid dispersions. Drug Dev. Ind. Pharm. 31, 473–489.
Koningsveld, R., Stockmayer, W.H., Nies, E., 2001. Polymer Phase Diagrams. Oxford University Press, New York.
Leuner, C., Dressman, J., 2000. Improving drug solubility for oral delivery using solid dispersions. Eur. J. Pharm. Biopharm. 50, 47–60.
Marsac, P.J., Shamblin, S.L., Taylor, L.S., 2006. Theoretical and practical approaches for prediction of drug–polymer miscibility and solubility. Pharm. Res. 23, 2417–2426.
Marsac, P.J., Li, T.L., Taylor, L.S., 2009. Estimation of drug–polymer miscibility and solubility in amorphous solid dispersions using experimentally determined interaction parameters. Pharm. Res. 26, 139–151.
Marsac, P.J., Rumondor, A.C.F., Nivens, D.E., Kestur, U.S., Stanciu, L., Taylor, L.S., 2010. Effect of temperature and moisture on the miscibility of amorphous dispersions of felodipine and poly(vinyl pyrrolidone). J. Pharm. Sci. 99, 169–185.
Mohan, R., Lorenz, H., Myerson, A.S., 2002. Solubility measurement using differential scanning calorimetry. Ind. Eng. Chem. Res. 41, 4854–4862.
Qian, F., Huang, J., Hussain, M.A., 2010. Drug–polymer solubility and miscibility: stability consideration and practical challenge in amorphous solid dispersion development. J. Pharm. Sci. 99, 2941–2947.
Rubinstein, M., Colby, R.H., 2003. Polymer Physics. Oxford University Press, New York.
Rumondor, A.C.F., Marsac, P.J., Stanford, L.A., Taylor, L.S., 2009a. Phase behavior of poly(vinylpyrrolidone) containing amorphous solid dispersions in the presence of moisture. Mol. Pharm. 6, 1492–1505.
Rumondor, A.C.F., Ivanisevic, I., Bates, S., Alonzo, D.E., Taylor, L.S., 2009b. Evaluation of drug–polymer miscibility in amorphous solid dispersion systems. Pharm. Res. 26, 2523–2534.
Rumondor, A.C.F., Stanford, L.A., Taylor, L.S., 2009c. Effects of polymer type and storage relative humidity on the kinetics of felodipine crystallization from amorphous solid dispersions. Pharm. Res. 26, 2599–2606.
Serajuddin, A.T.M., 1999. Solid dispersion of poorly water-soluble drugs: early promises, subsequent problems, and recent breakthroughs. J. Pharm. Sci. 88, 1058–1066.
Six, K., Murphy, J., Weuts, I., Craig, D.Q.M., Verreck, G., Peeters, J., Brewster, M., Van den Mooter, G., 2003. Identification of phase separation in solid dispersions of itraconazole and Eudragit E100 using microthermal analysis. Pharm. Res. 20, 135–138.
Strobl, G., 2007. The Physics of Polymers, 3rd edition. Springer, Berlin.
Sun, Y., Tao, J., Zhang, G.G.Z., Yu, L., 2010. Solubilities of crystalline drugs in polymers: an improved analytical method and comparison of solubilities of indomethacin and nifedipine in PVP, PVP/VA, and PVAc. J. Pharm. Sci. 99, 4023–4031.
Tao, J., Sun, Y., Zhang, G.G.Z., Yu, L., 2009. Solubility of small-molecule crystals in polymers: D-mannitol in PVP, indomethacin in PVP/VA, and nifedipine in PVP/VA. Pharm. Res. 26, 855–864.
Vasanthavada, M., Tong, W.Q., Joshi, Y., Kislalioglu, M.S., 2005. Phase behavior of amorphous molecular dispersions II: role of hydrogen bonding in solid solubility and phase separation kinetics. Pharm. Res. 22, 440–448.

Vasconcelos, T., Sarmento, B., Costa, P., 2007. Solid dispersions as strategy to improve oral bioavailability of poor water soluble drugs. Drug Discov. Today 12, 1068–1075.

Wiranidchapong, C., Tucker, I.G., Rades, T., Kulvanich, P., 2008. Miscibility and interactions between 17β-estradiol and Eudragit RS in solid dispersion. J. Pharm. Sci. 97, 4879–4887.

Yu, H.Q., Huang, A.B., Xiao, C.B., 2006. Characteristics of konjac glucomannan and poly(acrylic acid) blend films for controlled drug release. J. Appl. Polym. Sci. 100, 1561–1570.

Yu, L., 2001. Amorphous pharmaceutical solids: preparation, characterization and stabilization. Adv. Drug Deliv. Rev. 48, 27–42.